Stability of a Bose-Einstein condensate in an anharmonic trap

Barnali Chakrabarti,[1] T. K. Das,[2] and P. K. Debnath[3]
[1]*Department of Physics, Lady Brabourne College, P-1/2 Suhrawardy Avenue, Calcutta 700017, India*
[2]*Department of Physics, University of Calcutta, 92 A.P.C. Road, Calcutta 700009, India*
[3]*Santoshpur Sri Gouranga Vidyapith (H.S.), P.O. Kulitapara, Howrah 711312, India*
(Received 27 October 2008; revised manuscript received 24 January 2009; published 18 May 2009)

We study the stability of Bose-Einstein condensate (BEC) with repulsive and attractive interatomic interactions in a harmonic plus quartic trap $[V(r)=\frac{1}{2}m\omega^2r^2+\lambda r^4]$. We find that BEC with repulsive interaction becomes more stable for $\lambda>0$. For $\lambda<0$, we observe a different metastability of the condensate even when the scattering length is positive. For BEC with attractive interaction, we observe dramatic change in the stability factor $\frac{A_{cr}|a_{sc}|}{a_{ho}}$ due to the anharmonicity. The frequencies of the collective excitations are also modified by the atomic interaction and by the anharmonicity.

DOI: 10.1103/PhysRevA.79.053629 PACS number(s): 03.75.Hh

I. INTRODUCTION

In most of the experiments on ultracold alkali atomic vapors, the trapping potential is harmonic. However the choice of harmonic potential is very special and several recent experiments employ anharmonic traps which rapidly increase and become steeper at larger distances. A commonly used trap potential takes the form $V_{trap}(x)=\frac{1}{2}m\omega^2x^2+\lambda x^4$ in one-dimensional Bose-Einstein condensates (BECs). In the experiments of Stock and co-workers [1,2], a blue-detuned Gaussian laser directed along the axial direction makes the additional quartic confinement. They studied fast rotation of the ^{87}Rb condensate in such a quadratic plus quartic trap. In this trap configuration, one can easily increase the rotation frequency (Ω) above the trap frequency ($2\pi\nu$), which allows one to study the various phases of the gas: vortex creation, vortex excitation, and unstable phases. There are a lot of theoretical calculations mainly using the mean-field theory to study the quantized circular motion of the trapped condensate [3–10].

In the present study we are interested in the nonrotating condensate, where λ will be treated as a controllable parameter. We assume that λ is a small anharmonic parameter. For $\lambda>0$, the frequency is blueshifted and for $\lambda<0$, the frequency is redshifted. For the harmonic trapping, with repulsive interaction [for which s-wave scattering length (a_{sc}) is positive], the condensate is always stable for any number of bosons. However if two-body forces are attractive ($a_{sc}<0$), the gas tends to increase its density in the center of the trap. Naturally a collapse is expected when the number of bosons exceeds a critical value A_{cr}. For a spherical trap the onset of collapse is determined by the stability factor $k=\frac{A_{cr}|a_{sc}|}{a_{ho}}$, where $a_{ho}=\sqrt{\frac{\hbar}{2\pi m\nu}}$ is the oscillator length. The mean-field theory gives $k=0.575$ [11], whereas the experimental result is $k=0.459\pm0.012\pm0.054$ [12]. The many-body Schrödinger equation predicts $k=0.457$ [13,14] for a purely harmonic trap. Low-energy collective excitations in a harmonic trap with spherical and axial symmetry have also been calculated by different theoretical methods [11,15]. Recently collective excitations in anharmonic traps have been investigated and it has been observed that the frequency shifts of different excitation modes are significant when the atomic interaction is strong [16]. The stability of excited states of condensate in an anharmonic trap has also been studied [16]. However these authors considered either one-dimensional or effectively one-dimensional BEC with repulsive interaction only. Thus, further theoretical studies of three-dimensional condensate in anharmonic traps with both attractive and repulsive two-body forces remain to be done.

In the present work we find that the distortion produced by λ in the trap significantly affects the stability of the condensate. For repulsive interaction with $\lambda>0$, the effective potential in the hyper-radial space, in which the condensate is confined, becomes shifted upward and becomes steeper at large distances from the center of the cloud. Energies of the ground state and higher excitations are shifted upward. In general we find that stability increases when switching from a harmonic to an anharmonic potential with $\lambda>0$. For $\lambda<0$ we find the condensate to be metastable even when the interatomic interaction is repulsive. In this case, the condensate will have a finite decay probability of tunneling out to a noncondensed Bose gas. More drastic effect has been seen for negative scattering lengths, which correspond to attractive interactions. We find that the distortion makes the instability quicker and sets up new critical stability factor k. For the repulsive BEC we consider ^{87}Rb atoms with $a_{sc}=0.004\,33$ oscillator units (o.u.), which corresponds to the JILA experiment. For the attractive BEC we consider ^{85}Rb atoms with tunable interaction (scattering length tuned by Feshbach resonance) following the experiment by Roberts *et al.* [12].

The paper is organized as follows. In Sec. II we present the approximation used to solve the many-body Schrödinger equation for large number of trapped bosons. In Sec. III we discuss our results and conclusions are drawn in Sec. IV.

II. METHODOLOGY

Early theoretical studies on BEC were based on the mean-field approximation which results in the Gross-Pitaveskii (GP) equation for contact two-body interaction [11]. In the mean-field approximation the total condensate wave function is taken as a product of single-particle wave functions. Thus the effect of atomic correlation is completely ignored. It was

pointed out by several authors [17–19] that mean-field approximation is inadequate especially for the attractive condensate for the following reasons. First, for the attractive interaction, the atoms come closer and closer, making the central density of atomic cloud high. Hence one can no longer ignore the effect of atomic correlations. Second, the presence of an essential singularity at $r \to 0$ for the attractive contact interaction makes the Hamiltonian unbound from below. Naturally a full quantum many-body Schrödinger equation (with a realistic interaction, which should be strongly repulsive for $r \to 0$) is called for. In our study, we solve the many-body Schrödinger equation by the potential-harmonic-expansion method (PHEM), which basically uses a truncated basis set, keeping all two-body correlations. This is perfectly justified for the dilute condensate. Thus, in our method, we go beyond the mean-field approximation.

The basic idea of the PHEM is presented briefly below. The details can be found in Refs. [19–22]. After elimination of the center-of-mass motion, the Hamiltonian for $A=N+1$ identical trapped bosons is

$$H = \sum_{i=1}^{N} \nabla_{\vec{\zeta}_i}^2 + V_{\text{trap}} + V_{\text{int}}(\vec{\zeta}_1, \ldots, \vec{\zeta}_N), \tag{1}$$

where V_{trap} is the externally applied harmonic plus quartic trap. The set of N Jacobi vectors $\{\vec{\zeta}_1, \ldots, \vec{\zeta}_N\}$ describes the relative motion and V_{int} is the sum of all pairwise interactions. Hyperspherical-harmonic-expansion method (HHEM) is an *ab initio* many-body tool used to solve the many-body Schrödinger equation. The hyperspherical variables are constituted by the hyper-radius r and $(3N-1)$ hyperangles [$2N$ spherical polar angles $\{(\vartheta_j, \varphi_j), j=1,N\}$ associated with N Jacobi vectors and $(N-1)$ hyperangles $\{\phi_2, \phi_3, \ldots, \phi_N\}$ giving their relative lengths]. The total wave function is expanded in the complete set of hyperspherical-harmonic (HH) basis. The HH is the eigenfunction of the $3N$-dimensional hyperorbital angular momentum operator and has the form [20]

$$Y_{|\mathcal{L}|} = Y_{l_1 m_1}(\vartheta_1, \varphi_1) \prod_{j=2}^{N} Y_{l_j m_j}(\vartheta_j, \varphi_j)\, {}^{(j)}P_{\mathcal{L}_j}^{l_j \mathcal{L}_{j-1}}(\phi_j), \tag{2}$$

where $Y_{lm}(\omega)$ is a spherical harmonic and the function ${}^{(j)}P_{\mathcal{L}_j}^{l_j \mathcal{L}_{j-1}}(\phi_j)$ is expressed in terms of Jacobi polynomials [20]. The symbol $[\mathcal{L}]$ is a concise notation for the set of $(3N-1)$ quantum numbers [$2N$ orbital and azimuthal $\{(l_j m_j), j=1,2,\ldots,N\}$ and $(N-1)$ hyperspherical $\{n_j, j=2,\ldots,N;\ n_1=0\}$] quantum numbers. Due to the large degeneracy of the HH basis, HHEM is severely restricted to three-body systems only. Thus, although HHEM is a complete many-body approach, including *all* correlations, it cannot be applied to a typical BEC containing a large number of bosons. However, in a typical experimentally achieved BEC, the interparticle separation is very large compared with both the ranges of interatomic interactions and $|a_{\text{sc}}|$. Hence three- and higher-body correlations in the condensate wave function can be safely ignored [11,19,22]. In 1983 Fabre de la Ripelle [21] proposed an approximate but manageable way to include all two-body correlations by choosing a subset of the full HH basis, which is necessary and sufficient for the expansion of the two-body potential $V(r_{ij})$ to expand the (ij) Faddeev component. This subset is called potential harmonics (PHs) and is clearly independent of the coordinates of the $(A-2)$ noninteracting particles. Closed analytic expressions are possible for the PH basis [21]. Choosing $\vec{\zeta}_N = \vec{r}_{ij}$, we have $\{l_k=0,\ m_k=0,\ n_k=0;\ k=1,\ N-1\}$. The full wave function is then written as a sum of all pairwise Faddeev components. Since only two-body correlations are relevant, the Faddeev component for the (i,j) interacting pair is a function only of $\vec{r}_{ij}$ and r. Hence it can be expanded in the PH appropriate for the (ij) partition. The expansion in the PH basis offers a complete description of two-body correlation and ignores three- and higher-body correlations. The contribution to the total orbital and grand orbital angular momenta comes only from the interacting pair.

The PH basis function has an analytic expression [21]

$$\mathcal{P}_{2K+l}^{l,m}(\Omega_N^{(ij)}) = Y_{lm}(\omega_{ij})\, {}^{(N)}P_{2K+l}^{l,0}(\phi)\mathcal{Y}_0(D-3), \quad D=3N. \tag{3}$$

$\Omega_N^{(ij)}$ represents the set of hyperangles corresponding to the (i,j) partition $(\vec{\zeta}_N = \vec{r}_{ij})$ and $\mathcal{Y}_0(3N-3)$ is the HH of order zero in the $(3N-3)$-dimensional space spanned by $\{\vec{\zeta}_1, \ldots, \vec{\zeta}_{N-1}\}$ Jacobi vectors. ϕ is the hyperangle given by $r_{ij} = r\cos\phi$. The set of $(3N-1)$ quantum numbers of HH is now reduced to *only three* for any number of particles. These are

$$l_1 = l_2 = \cdots = l_{N-1} = 0, \quad l_N = l, \tag{4}$$

$$m_1 = m_2 = \cdots = m_{N-1} = 0, \quad m_N = m, \tag{5}$$

$$n_2 = n_3 = \cdots = n_{N-1} = 0, \quad n_N = K. \tag{6}$$

Hence the three independent quantum numbers are $\mathcal{L} = 2K + l$, $L=l$, and $M=m$. As there are only three active angle variables for any N, the numerical difficulty in the imposition of symmetry and calculation of potential matrix element is tremendously simplified. The full wave function Ψ is decomposed into Faddeev components

$$\Psi = \sum_{ij>i}^{A} \psi_{ij}, \tag{7}$$

and ψ_{ij} is expanded in the appropriate PH basis,

$$\psi_{ij} = r^{-[(3N-1)/2]} \sum_{K} \mathcal{P}_{2K+l}^{lm}(\Omega_N^{(ij)}) u_K^l(r). \tag{8}$$

The two-body Faddeev component satisfies

$$[T + V_{\text{trap}} - E]\psi_{ij} = -V(r_{ij}) \sum_{kl>k}^{A} \psi_{kl}. \tag{9}$$

Summing both sides over all (ij) pairs, we get back the full many-body Schrödinger equation.

But the convergence of the above expansion is slow, since the first term of the expansion basis is a constant and does not reflect the strong two-body repulsion for $r_{ij} \to 0$. We include a short-range correlation function $\eta(r_{ij})$ in the PH ex-

pansion to enhance the rate of convergence. Thus in the correlated-potential-harmonic-expansion method (CPHEM), Eq. (8) is replaced by

$$\psi_{ij} = r^{-[(3N-1)/2]} \sum_K \mathcal{P}^{lm}_{2K+l}(\Omega_N^{(ij)}) u^l_K(r)\, \eta(r_{ij}). \tag{10}$$

The need for such a correlation function can also be understood from the experimental context. In a typical BEC experiment the condensate is kept at a very low temperature and in very dilute condition. Hence only binary collision at almost zero kinetic energy is relevant, which is completely described in terms of the s-wave scattering length. Hence we obtain $\eta(r_{ij})$ as the zero-energy solution of (ij)-pair relative motion in the potential $V(\vec{r}_{ij})$,

$$-\frac{\hbar^2}{m}\frac{1}{r_{ij}^2}\frac{d}{dr_{ij}}\left(r_{ij}^2\frac{d\eta(r_{ij})}{dr_{ij}}\right) + V(r_{ij})\,\eta(r_{ij}) = 0. \tag{11}$$

The correlation function quickly attains its asymptotic form $C(1-\frac{a_{sc}}{r_{ij}})$ for large r_{ij}. The asymptotic normalization is chosen to make the wave function positive at large r_{ij} [13]. Substitution of Eq. (10) into the many-body Schrödinger equation and projection on a particular PH gives a set of coupled differential equations,

$$\left[-\frac{\hbar^2}{m}\frac{d^2}{dr^2} + V_{\text{trap}} + \frac{\hbar^2}{mr^2}\{\bar{\mathcal{L}}(\bar{\mathcal{L}}+1) + 4K(K+\alpha+\beta+1)\} - E\right] \times U_{Kl}(r)\Sigma_{K'} f_{Kl} V_{KK'}(r) f_{K'l} U_{K'l}(r) = 0, \tag{12}$$

where $V_{\text{trap}} = \frac{1}{2}m\omega^2 r^2 + \lambda r^4$ is the externally applied trapping potential. $U_{Kl}(r) = f_{Kl} u^l_K(r)$, $\bar{\mathcal{L}} = l + \frac{3A-6}{2}$, $\alpha = \frac{3A-8}{2}$, $\beta = l + \frac{1}{2}$, and f_{Kl} is a constant representing overlap of the PH for interacting partition with the full set, which is given in Ref. [21]. The potential matrix element $V_{KK'}(r)$ is given by

$$V_{KK'}(r) = (h_K^{\alpha\beta} h_{K'}^{\alpha\beta})^{-1/2} \int_{-1}^{+1} P_K^{\alpha\beta}(z) \times V\left(r\sqrt{\frac{1+z}{2}}\right) P_{K'}^{\alpha\beta}(z)\, \eta\left(r\sqrt{\frac{1+z}{2}}\right) W_l(z)\, dz. \tag{13}$$

Here $h_K^{\alpha\beta}$ and $W_l(z)$ are, respectively, the norm and weight function of the Jacobi polynomial $P_K^{\alpha\beta}(z)$ [23]. Numerical procedure used to handle the extreme rapid variation in $W_l(z)$ near $z=-1$, especially for large A, and the technique used to calculate the integrals with large precision even when $A = 14\,000$, are well described in previous works [13,19]. The set of CDEs is solved by hyperspherical adiabatic approximation [24,25], in which potential matrix together with hypercentrifugal repulsion is diagonalized for a fixed value of r. The lowest eigenvalue gives the lowest eigenpotential, $\omega_0(r)$, as a parametric function of r. This $\omega_0(r)$ is the collective potential as a function of the hyper-radius (r), in which the condensate moves in the hyper-radial space. The energy and wave function of the system are then obtained by solving the adiabatically separated hyper-radial equation for the collective motion with $\omega_0(r)$ as the effective potential.

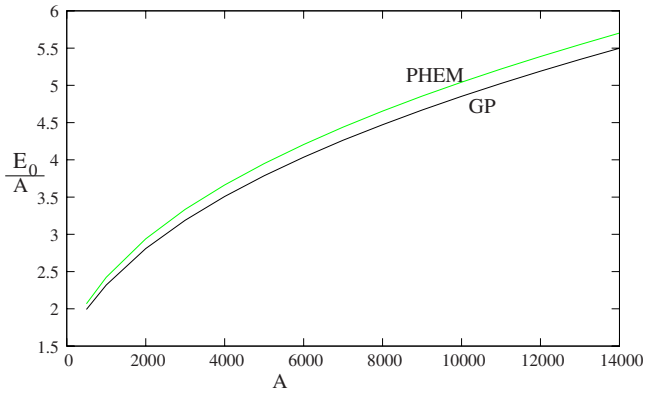

FIG. 1. (Color online) Plots of ground-state energy per particle in o.u. for ^{87}Rb atoms (with $a_{sc}=0.004\,33$ o.u.) as a function of A, calculated by PHEM and GP equation.

III. RESULTS

The interatomic potential has been chosen to be the van der Waals potential with a hard core of radius r_c, viz., $V(r_{ij})=\infty$ for $r_{ij} \le r_c$ and $=-\frac{C_6}{r_{ij}^6}$ for $r_{ij} > r_c$. The strong short-range repulsion is parametrized by the hard core. The strength (C_6) is known for a given type of atom. We use o.u. corresponding to the trap frequency (ν) of the JILA experiment with ^{87}Rb atoms [26]. For Rb atoms, $C_6 = 6.4898 \times 10^{-11}$ o.u. In the limit of $C_6 \to 0$, the potential becomes a hard sphere and r_c coincides with the s-wave scattering length a_{sc}. For the potential including the long-range part, a tiny change in r_c may cause an enormous change in a_{sc}, including sign [27]. As r_c decreases from a large value, a_{sc} decreases, and at a particular critical value of r_c, it passes through an infinite discontinuity from $-\infty$ to $+\infty$ [13]. Thereafter the potential supports a two-body bound state. This pattern repeats as r_c decreases further. Positive values of a_{sc} correspond to repulsive potential, whereas negative a_{sc} values correspond to attractive potential. Thus minute tuning of r_c can cause the effective potential to change from attractive to repulsive. In the laboratory this is achieved by Feshbach resonances [12,28].

A. Repulsive condensate with $\lambda > 0$

For the repulsive BEC we consider the condensate containing ^{87}Rb atoms. We choose the scattering length $a_{sc} = 0.004\,33$ o.u. at trap frequency $\nu = 77.78$ Hz. These parameters correspond to the JILA experiment [26]. In Fig. 1 we plot the ground-state energy per particle $(\frac{E_0}{A})$ versus A, for condensates containing up to 14 000 atoms in the spherical harmonic trap $(\lambda=0)$. The value of r_c is chosen to be 1.21×10^{-3} o.u., which gives $a_{sc}=0.004\,33$ o.u. from the asymptotic $\eta(r_{ij})$, having one node. In the same figure, we also present the results obtained from the GP equation, for comparison.

In Fig. 2, the ground-state energy per particle, $\frac{E_0}{A}$, is plotted as a function of anharmonicity parameter λ, for small distortions and for selected number of particles in the condensate. The effect of anharmonicity is quite prominent even

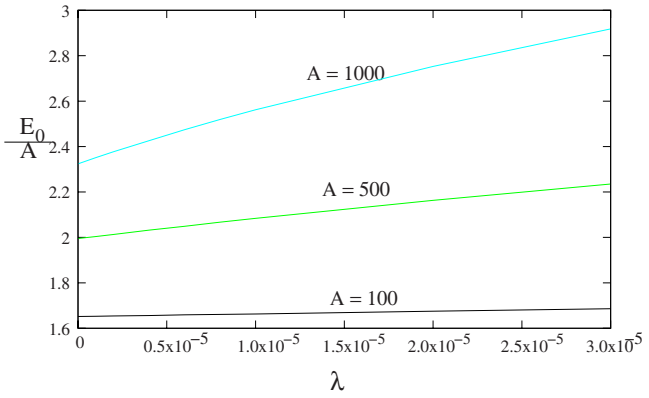

FIG. 2. (Color online) Plots of ground-state energy per particle in o.u. as a function of anharmonicity λ, for different indicated values of A.

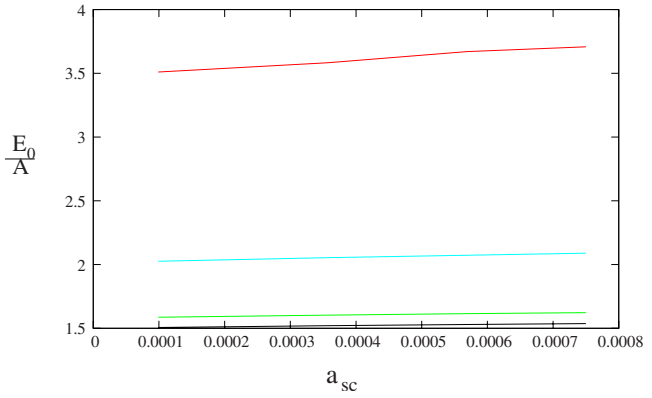

FIG. 4. (Color online) Plot of ground-state energy per particle in o.u. for $A=100$ bosons, as a function of a_{sc} for different λ (=0.01, 0.001, 0.0001, and 0.0 in o.u. respectively from top to bottom).

when λ is quite small and $\frac{E_0}{A}$ gradually increases for $\lambda>0$. The effect is larger for larger A. This can also be visualized from Fig. 3, where we plot the lowest eigenpotential, $\omega_0(r)$ for harmonic and anharmonic ($\lambda=0.0001$ o.u.) trappings for $A=500$. In our many-body picture, ω_0 is the effective potential in which the condensate is trapped in the hyper-radial space. For $\lambda=0$, ω_0 is roughly harmonic, but shifted upward due to the repulsive interatomic interaction. As the condensate is very dilute, the effect of harmonic trapping is dominating. Now for $\lambda=0.0001$ o.u., ω_0 becomes upwardly shifted, the shift being significant. It also becomes tighter as the quartic term grows much faster than the quadratic term for larger distances from the center of the atomic cloud. This causes stronger binding and naturally ground-state energy will increase. In Ref. [2], the strength of quartic admixture was $\lambda=10^{-3}$.

The effect of larger anharmonicity is shown in Fig. 4, where we plot $\frac{E_0}{A}$ as a function of interaction strength (a_{sc}) for chosen values of λ (=0, 10^{-4}, 10^{-3}, and 10^{-2} o.u.) and a fixed value of A (=100). The energy per particle increases slowly for $\lambda=0$. For small values of λ (10^{-4} and 10^{-3} o.u.) the curves are nearly parallel to the $\lambda=0$ curve, indicating that the effect of anharmonicity is small. This is because the chosen values of scattering length are quite small and the condensate is extremely dilute. But the effect is appreciable for $\lambda=0.01$, and ground-state energy significantly increases even when the weakly interacting condensate is very dilute.

For the same range of interatomic interaction and same A, we plot the lowest excitation frequency, $\omega_M=(E_1-E_0)/\hbar$, as a function of a_{sc} in Fig. 5. For $\lambda=0$, the frequency of the lowest breathing oscillation is nearly double the external trap frequency, which is 2 in our chosen unit. For $\lambda=0.0001$, the frequency is shifted to 2.31 and for $\lambda=0.001$, it is 3.63, for a noninteracting condensate ($a_{sc}=0$).

The results for larger scattering length ($a_{sc}=0.004\,33$ o.u.) and for larger anharmonicity are shown in Fig. 6, where $\frac{E_0}{A}$ is plotted against A for chosen values of λ. The effect is quite large due to magnified effects of the interatomic interaction.

B. Repulsive condensate with $\lambda<0$

Drastic effects are seen for $\lambda<0$, for which the excitation frequency is redshifted. In Fig. 7, the effective potential is plotted as a function of r, for $A=500$, $\lambda=-0.000\,02$ o.u., and $a_{sc}=0.004\,33$ o.u. We observe dramatic change in the effective potential, which poses the important question of

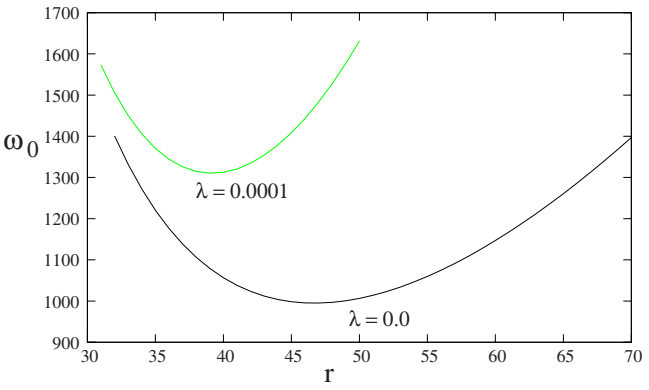

FIG. 3. (Color online) Plot of effective potential (lowest eigenpotential) $\omega_0(r)$ in o.u. against r for $A=500$ bosons for harmonic (lower curve) and anharmonic traps (upper curve).

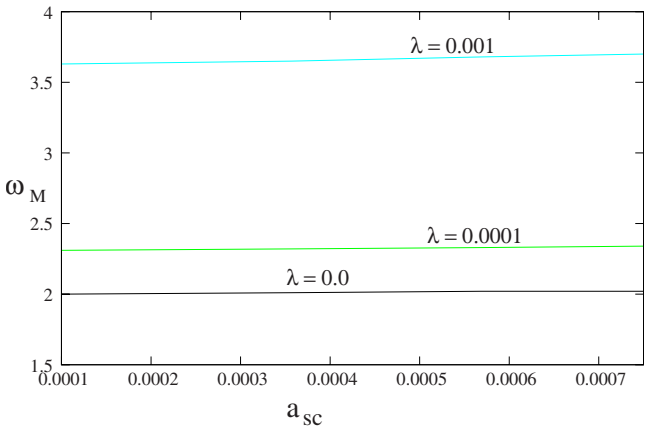

FIG. 5. (Color online) Lowest excitation frequency of breathing mode (ω_M) in o.u. for $A=100$ bosons as a function of a_{sc} for different λ as indicated in figure.

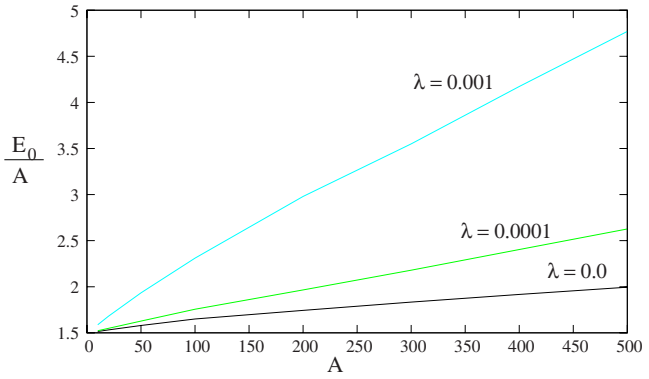

FIG. 6. (Color online) Plot of ground-state energy per particle in o.u. as a function of A for different anharmonicity as indicated in figure.

stability of the condensate even when the scattering length is positive.

From Fig. 7 we see that the condensate has a metastability, but of a nature different from the usual one (harmonic and $a_{sc}<0$). It has a large tunneling probability to tunnel out of the condensate to larger distances, giving rise to a noncondensed Bose gas. The tunneling probability can be calculated using the semiclassical WKB approximation. In the case of an attractive condensate in a harmonic trap, a very deep well appears on the left side of the metastable region (MSR) [13] and just before collapse (A slightly less that A_{cr}) the metastable condensate tunnels *inward* and settles down to a lower-energy state within the well, forming bound clusters. The released binding energy causes heating. In that case $\omega_0(r)$ increases steeply on the right side and the condensate will decay only through the intermediate barrier near origin, forming bound clusters of atoms. For positive a_{sc}, atoms try to be further away from each other. When λ becomes negative, a metastable region and a barrier *on the right of the MSR* appear, the effective potential decreasing thereafter. Hence the condensate will easily tunnel out of the trap (see Fig. 7). But this time there will be no cluster formation; the atoms will escape *outward* from the metastable trap and form a dilute noncondensed Bose gas. Thus we fail to get a permanently stable condensate for $\lambda<0$, $a_{sc}>0$. As λ decreases

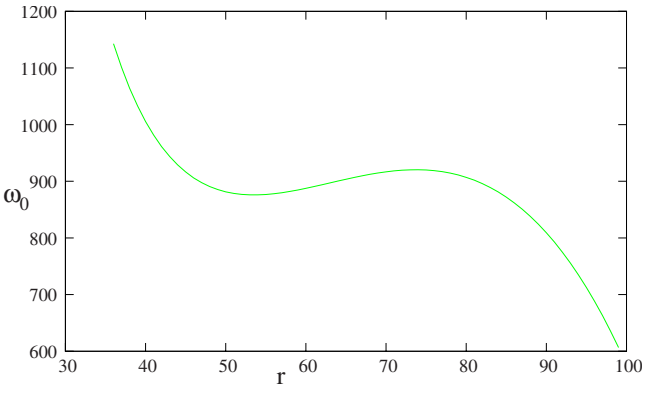

FIG. 7. (Color online) Plot of effective potential $\omega_0(r)$ against r in o.u. for $A=500$ bosons in anharmonic trap with $\lambda=-0.000\ 02$ o.u.

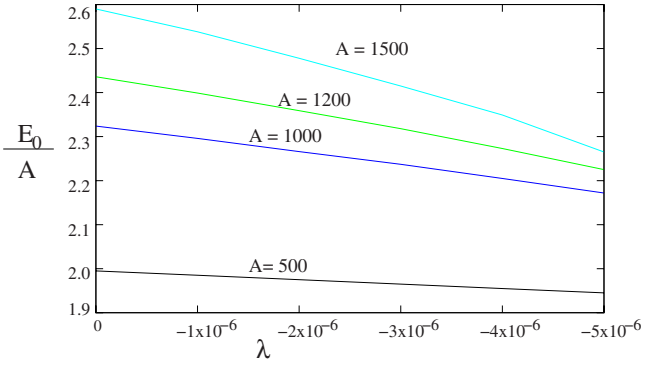

FIG. 8. (Color online) Plots of ground-state energy per particle (in o.u.) as a function of λ for different indicated particle numbers.

(for a given A and a fixed positive a_{sc}), tunneling probability increases and lifetime of the metastable condensate decreases. In this case, there will be a critical value of λ at which the metastable region of Fig. 7 just disappears, beyond which no metastable condensate is possible. Note that we tacitly assume that the external field producing the anharmonic trapping is of finite spatial extent. Otherwise even a small negative value of λ will exclude a metastable solution. This collapse occurs for less negative values of λ, as A increases. For example, for $A=1000$, collapse occurs at $\lambda=-0.000\ 01$ and for $A=1200$ collapse sets in at $\lambda=-8\times10^{-6}$ (both for $a_{sc}=0.004\ 33$ o.u.).

In Fig. 8, $\frac{E_0}{A}$ is plotted against negative λ for $a_{sc}=0.004\ 33$ o.u. and selected number of particles. The ground-state energy per particle rapidly decreases even for very small change in λ and the effect gets enhanced for larger A.

C. Attractive condensate with $\lambda>0$

Next we study the stability of an attractive condensate in a positive anharmonic trap. The commonly studied instability arises from attractive interactions in a harmonic trap. For our purpose, we choose the ^{85}Rb condensate in the JILA trap where the controlled collapse was observed in the harmonic trap. In this experiment [12,28] Feshbach resonance was used to tune different negative scattering lengths and then find the critical number which determines the stability factor. In our many-body approach we just tune the cutoff radius to make the condensate more attractive, i.e., making a_{sc} more negative. In Table I we present the chosen a_{sc} values [12,28] and the corresponding cutoff radii r_c. For chosen values of a_{sc} (negative) and λ (positive) we calculate $\omega_0(r)$ for increasing number of particles. The curve has the same pattern as that for an attractive condensate in a harmonic trap (see Fig. 4 of Ref. [13]). For smaller values of A, as r increases from zero, $\omega_0(r)$ decreases sharply from a large positive value, passing through a finite minimum, increases sharply again to an intermediate finite barrier, decreases again, reaching a local minimum, and then increases with r. The last well is the MSR in which the attractive condensate resides. For large r, $\omega_0(r)$ increases more steeply as positive λ increases. For fixed negative a_{sc} and positive λ, the MSR gradually shrinks

TABLE I. Selected values of a_{sc} reported by Roberts *et al.* [12] to study the controlled collapse of ^{85}Rb atoms. The potential is van der Waals with $C_6=6.4898\times10^{-11}$ o.u. The required values of r_c are obtained from the two-body solution in the zero energy.

a_{sc} (o.u.)	r_c (o.u.)
-1.836×10^{-4}	1.3955×10^{-3}
-1.7901×10^{-4}	1.3960×10^{-3}
-1.3885×10^{-4}	1.4003×10^{-3}
-9.7538×10^{-5}	1.4050×10^{-3}
-7.2293×10^{-5}	1.4080×10^{-3}

with increasing A, and finally at a critical value $A=A_{cr}$, it disappears completely. The condensate is metastable for $A<A_{cr}$ and becomes unstable for $A=A_{cr}$. The critical stability factor is again given by $k=\frac{A_{cr}|a_{sc}|}{a_{ho}}$, where a_{ho} is the oscillator length. For a fixed λ, we calculate A_{cr} for each of the chosen negative values of a_{sc} and plot $\frac{1}{A_{cr}}$ against $|a_{sc}|$ in Fig. 9.

The points are nearly on a straight line for a fixed λ. From a linear least-squares fit, we calculate the slope of the straight lines. The slope of each graph determines the critical stability factor for different anharmonicities. In Table II, we present the value of k for different distortions λ. The effect is really dramatic. The anharmonicity causes quicker collapse. As a_{sc} becomes more negative, the atoms come closer due to attractive interaction. Furthermore, with increasing positive λ, the effective potential becomes steeper in the outer region, forcing the atoms toward the center of the atomic cloud, tending to increase the central density. Both these effects cause shrinking of the MSR and thus collapse sets in quicker.

The situation will be more interesting for the case with negative λ. In Fig. 10 we have shown the effective potential with $a_{sc}=-1.832\times10^{-4}$ o.u. and $\lambda=-7\times10^{-6}$. Here the metastable condensate is now bounded by the two neighbor barriers. The left-side barrier is the effect of negative scattering length as one gets for the attractive condensate in the usual case of harmonic trapping, whereas the right-side barrier is the effect of negative anharmonicity which basically

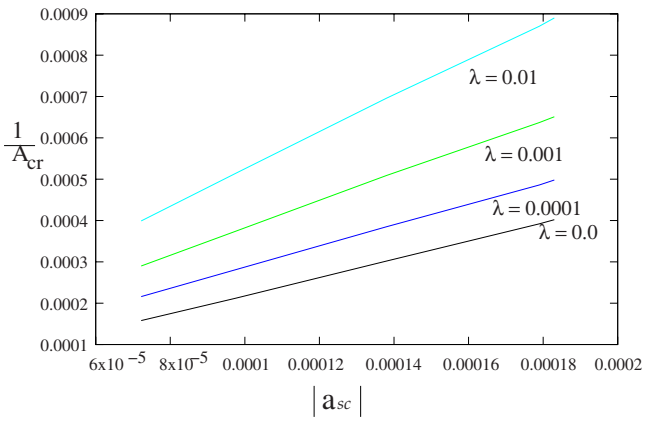

FIG. 9. (Color online) Plots of $\frac{1}{A_{cr}}$ against $|a_{sc}|$ for a condensate of ^{87}Rb atoms with tunable interaction for different indicated values of λ (in o.u.).

TABLE II. Calculated stability factors for the above set of a_{sc} values with different anharmonicities in the external trap.

Distortion (λ)	$k=\frac{A_{cr}\|a_{sc}\|}{a_{ho}}$	Experimental value [12]
0.0	0.453	$0.459\pm0.012\pm0.054$
0.0001	0.394	
0.001	0.307	
0.01	0.226	

corresponds to finite optical trap. Naturally in such situation the metastable condensate will have the probability to tunnel out the trap through both the barriers. Figure 10 corresponds to A=2000 bosons in the trap. We have checked that increasing the value of $\lambda\simeq-1\times10^{-4}$, the barrier on the right side quickly decreases even when A is quite small ($\simeq100$). Now increasing $A=300$, we observed that the metastability just disappears and the condensate will leak completely as expected, whereas keeping λ fixed, if we tune a_{sc} to more negative values, the metastable condensate now will leak through the left-side barrier. As there are two competing factors in this case, depending on the most dominating part, the form of the effective potential will change abruptly.

IV. CONCLUSIONS

We have investigated the properties of Bose-Einstein condensates in a harmonic plus quartic trap for both attractive and repulsive interatomic interactions. The coefficient of the quartic term (λ) has both positive and negative values. For positive λ, the trap becomes steeper. As a consequence energy per particle and excitation energy increase with increasing positive λ and positive a_{sc}, as expected. Interesting features are observed for negative λ. For a finite extent of the trap and for small negative λ, energy per particle decreases as expected. For larger negative λ, but repulsive interaction ($a_{sc}>0$), a metastable region is formed in the effective potential $\omega_0(r)$, permitting leakage of particles to larger distances away from the condensate cloud. The escaped atoms form a noncondensed Bose gas with no increase in tempera-

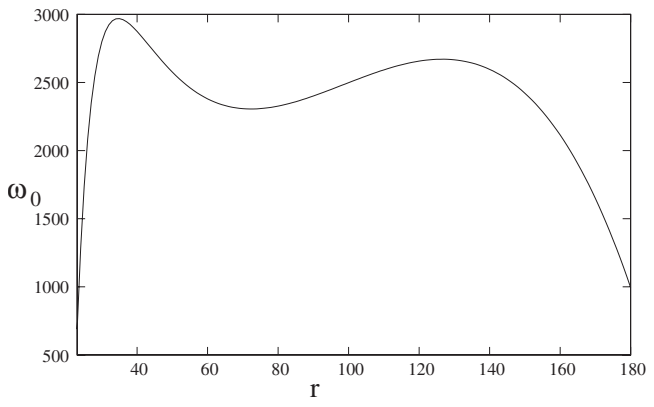

FIG. 10. Plot of effective potential $\omega_0(r)$ against r in o.u. for $A=2000$ bosons in an anharmonic trap with $\lambda=-7\times10^{-6}$ and $a_{sc}=-1.832\times10^{-4}$ o.u.

ture. This metastability is very different from the metastable condensates for attractive interaction ($a_{sc}<0$), where atoms from the condensate tunnel through an intermediate barrier, into a deep narrow well near the center, forming clusters and heating the cluster gas by the released binding energy.

The situation is also interesting for attractive condensates ($a_{sc}<0$) with positive λ. Attractive interaction in a harmonic trap produces a metastable region in the effective potential. With increase of particle number, the metastable region shrinks and at a critical value ($=A_{cr}$), it just disappears signaling a collapse of the metastable condensate. For positive λ, $\omega_0(r)$ becomes steeper in the outer region, forcing atoms inward. On the other hand as A increases for a negative a_{sc}, atoms tend to come closer together toward the origin. Both the effects being in the same direction, collapse occurs sooner and the critical stability factor decreases as positive λ increases.

ACKNOWLEDGMENTS

This work was supported by a grant from the Department of Science and Technology (DST) [Fund No. SR/S2/CMP/0059(2007)], Government of India, under a research project.

[1] S. Stock, V. Bretin, F. Chevy, and J. Dalibard, Europhys. Lett. **65**, 594 (2004).
[2] V. Bretin, S. Stock, Y. Seurin, and J. Dalibard, Phys. Rev. Lett. **92**, 050403 (2004).
[3] A. L. Fetter, Phys. Rev. A **64**, 063608 (2001).
[4] Xavier Blanc and N. Rougerie, Phys. Rev. A **77**, 053615 (2008).
[5] S. Kling and A. Pelster, Phys. Rev. A **76**, 023609 (2007).
[6] G. M. Kavoulakis and G. Baym, New J. Phys. **5**, 51 (2003).
[7] T. P. Simula, A. A. Penckwitt, and R. J. Ballagh, Phys. Rev. Lett. **92**, 060401 (2004).
[8] A. D. Jackson, G. M. Kavoulakis, and E. Lundh, Phys. Rev. A **69**, 053619 (2004).
[9] A. Collin, Phys. Rev. A **73**, 013611 (2006).
[10] H. Fu and E. Zaremba, Phys. Rev. A **73**, 013614 (2006).
[11] F. Dalfovo, S. Giorgini, L. P. Pitaevskii, and S. Stringari, Rev. Mod. Phys. **71**, 463 (1999).
[12] J. L. Roberts, N. R. Claussen, S. L. Cornish, E. A. Donley, E. A. Cornell, and C. E. Wieman, Phys. Rev. Lett. **86**, 4211 (2001); J. L. Roberts, N. R. Claussen, J. P. Burke, C. H. Greene, E. A. Cornell, and C. E. Wieman, *ibid.* **81**, 5109 (1998).
[13] A. Kundu, B. Chakrabarti, T. K. Das, and S. Canuto, J. Phys. B **40**, 2225 (2007).
[14] T. K. Das, A. Kundu, S. Canuto, and B. Chakrabarti, Phys. Lett. A **373**, 258 (2008).
[15] A. Biswas and T. K. Das, J. Phys. B **41**, 231001 (2008).
[16] G. Q. Li, L. B. Fu, J. K. Xue, X. Z. Chen, and J. Liu, Phys. Rev. A **74**, 055601 (2006); D. A. Zezyulin, G. L. Alfimov, V. V. Konotop, and V. M. Perez-Garcia, *ibid.* **78**, 013606 (2008).
[17] S. Bargi, G. M. Kavoulakis, and S. M. Reimann, Phys. Rev. A **73**, 033613 (2006).
[18] S. Geltman, Chem. Phys. Lett. **418**, 163 (2006); J. Phys. B **37**, 315 (2004).
[19] T. K. Das, S. Canuto, A. Kundu, and B. Chakrabarti, Phys. Rev. A **75**, 042705 (2007).
[20] J. L. Ballot and M. Fabre de la Ripelle, Ann. Phys. (N.Y.) **127**, 62 (1980).
[21] M. Fabre de la Ripelle, Ann. Phys. (N.Y.) **147**, 281 (1983).
[22] T. K. Das and B. Chakrabarti, Phys. Rev. A **70**, 063601 (2004).
[23] M. Abramowitz and I. A. Stegun, *Handbook of Mathematical Functions* (Dover, New York, 1972), p. 773.
[24] T. K. Das, H. T. Coelho, and M. Fabre de la Ripelle, Phys. Rev. C **26**, 2281 (1982).
[25] J. L. Ballot, M. Fabre de la Ripelle, and J. S. Levinger, Phys. Rev. C **26**, 2301 (1982).
[26] M. H. Anderson *et al.*, Science **269**, 198 (1995).
[27] C. J. Pethick and H. Smith, *Bose-Einstein Condensation in Dilute Gases* (Cambridge University Press, Cambridge, England, 2001).
[28] S. L. Cornish, N. R. Claussen, J. L. Roberts, E. A. Cornell, and C. E. Wieman, Phys. Rev. Lett. **85**, 1795 (2000).